New Trends and Issues Proceedings on Advances in Pure and Applied Sciences

Issue 9, (2017) 41-51

www.propaas.eu
ISSN: 2547-880X

Selected Paper of Selected Paper of 3rd Global Conference on Material Sciences (GC-MAS-2017), 28-30 August 2017
Bahcesehir University Besiktas Campus, Istanbul, Turkey

Effect of physical and geometrical parameters on low-velocity impact response of sandwich beams with carbon nanotube reinforced face sheets

S. Jedari Salami [a]*, Department of Mechanical Engineering, Damavand branch, Islamic Azad University, Damavand, Iran

Suggested Citation:
Salami, S.J. (2017). Effect of physical and geometrical parameters on low-velocity impact response of sandwich beams with carbon nanotube reinforced face sheets. *New Trends and Issues Proceedings on Advances in Pure and Applied Sciences*. [Online]. 9, 41–51. Available from: www.propaas.eu

Selection and peer review under responsibility of Assist. Prof. Dr. Engin Baysen, Near East University, Nicosia, Cpyrus.

Abstract

The response of sandwich beam with carbon nanotube (CNT) reinforced composite face sheets and soft core when subjected to the action of an impacting mass is analysed theoretically. Contact force between the impactor and the beam is obtained using the conventional Hertz law. The field equations are derived via the Ritz based applied to the total energy of the system. The solution is obtained in the time domain by implementing the well-known Runge–Kutta method. After examining the validity of the present solution, the effects of distribution of CNTs, nanotube volume fraction, core-to-face sheet thickness ratio, initial velocity of the impactor and the impactor mass are studied in detail. Finally, it is concluded that, the highest peak contact force and the lowest indentation of the top face sheet belong to the sandwich beam with V-distribution figure of face sheet, followed by the uniformly distributed and Λ-ones, respectively.

Keywords: Carbon nanotube fibers, sandwich beam, soft core.

* ADDRESS FOR CORRESPONDENCE: **S. Jedari Salami,** Department of Mechanical Engineering, Damavand branch, Islamic Azad University, Damavand, Iran.
E-mail address: sattar.salami@aut.ac.ir / Tel.:+989-122-453-217

1. Introduction

Carbon nanotubes (CNTs) are known as a novel type of materials which have attracted increasing attention in recent years. These materials have remarkable physical and chemical properties such as high strength, high stiffness, high aspect ratio and very low density, which make them as a potential substance for the reinforcement of the composites. It is reported that Young's modulus of CNT may be more than 1 TPa, where its density is only 1.3 g/cm^3 [4]. CNTs can be single-walled CNT (SWCNT) or multi-walled CNT (MWCNT). SWCNT is in a cylindrical shape which is rolled seamlessly by a single sheet of graphene with ~1 nm diameter and length of order of centimetres. By contrast, MWCNT has an array of such cylinders formed concentrically and separated by 0.35 nm, similar to the basal plane separation in graphite with diameters from 2–100 nm and lengths of tens of microns [1]. A small weight percentage of the CNTs (2–5%) as the reinforcements in the composites, in comparison with using traditional carbon fibers, can considerably enhance the stiffness and strength of the composites [10]. On the other hand, adding more amount of CNTs to the composites can actually lead to the degradation of their mechanical properties.

Shen [8] showed that through a FG distribution of CNTs across the thickness of a rectangular plate, bending moments may be decreased significantly in comparison to the case of a plate with uniform distribution of CNTs. After the interesting results of this piece of work in 2009, various investigations are done to examine the mechanical and thermal responses of FG–CNTRC.

To date, only few studies regarding sandwich panels with FG–CNTRC face sheets are available in the literature.

Bending, free vibration and dynamic transient responses of a sandwich beam with polyurethane soft core and CNTRC face sheets were investigated by Jedari Salami [2–4]. As the above literature survey accepts, and to the best of author's knowledge, there is no work on the low velocity impact response of a sandwich panel with FG–CNTRC face sheets and soft core. In the present study, low velocity impact analysis of a sandwich beam with polyurethane soft core and CNTRC face sheets based on EHSAPT is investigated. The influences of distribution of CNTs, nanotube volume fraction, core-to-face sheet thickness ratio, initial velocity of the impactor and the impactor mass are studied.

2. Basic formulation

A sandwich beam is composed from two stiff thin face sheets separated by a relatively thick soft core (Figure 1). In this study, the two face sheets are made of CNTRCs where the SWCNT reinforcement is either uniformly distributed (UD) or FG in the thickness direction.

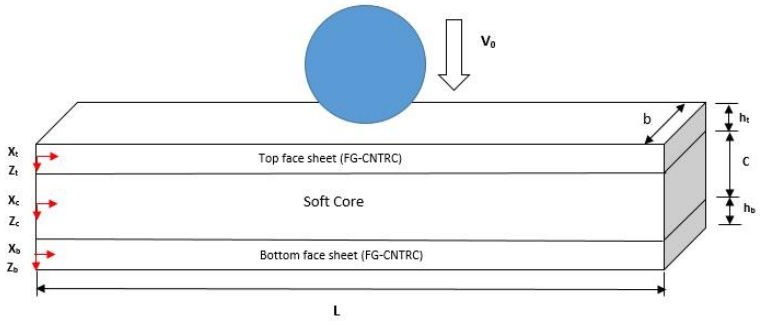

Figure 1. Description of the geometrical configuration for the sandwich beam

In this study, three different types of carbon nanotube reinforced beams which include a UD case and two different FG cases, namely FG-V and FG-Λ have been considered for each of the face sheets. As a convention, a FG-V sandwich beam is referred to a beam where the top face sheet is of FG-V type

and the bottom one is of FG-Λ. Also, the distribution pattern of face sheets for a FG-Λ sandwich beam is vice versa.

The effective material properties of the two-phase composites, mixture of CNTs and an isotropic polymer, can be estimated according to the modified rule of mixtures as previously discussed by Shen [9]. To this end, the conventional rule of mixture approach is modified by introduction of efficiency parameters as follows:

$$E_{11} = \eta_1 V_{CN} E_{11}^{CN} + V_m E^m \tag{1}$$

$$\frac{\eta_2}{E_{22}} = \frac{V_{CN}}{E_{22}^{CN}} + \frac{V_m}{E^m} \tag{2}$$

$$\frac{\eta_3}{G_{12}} = \frac{V_{CN}}{G_{12}^{CN}} + \frac{V_m}{G^m} \tag{3}$$

Where in the above equations, E_{11}^{CN}, E_{22}^{CN} and G_{12}^{CN} are the Young's modulus and shear modulus, respectively, of SWCNTs, E^m and G^m are associated properties of the matrix.

The coefficients η_1, η_2 and η_3 are the so-called efficiency parameters to account for the scale dependent material properties. Furthermore, in Eqs. (1)–(3), V_{CN} and V_m are the volume fractions of CNTs and matrix phase which satisfy the below condition. Mathematical definition of CNTs volume fraction in each case of distribution is given in Table 1.

$$V_{CN} + V_m = 1 \tag{4}$$

Table 1. Volume fraction of CNTs as a function of thickness coordinate for various cases of sandwich beams with CNTRC face sheets

CNTs distribution pattern	V_{CN} (top face sheet)	V_{CN} (bottom face sheet)
UD CNTRC	V_{CN}^*	V_{CN}^*
FG–V CNTRC	$2V_{CN}^*\left(0.5-\frac{z}{h_t}\right)$	$2V_{CN}^*\left(0.5+\frac{z}{h_b}\right)$
FG–Λ CNTRC	$2V_{CN}^*\left(0.5+\frac{z}{h_t}\right)$	$2V_{CN}^*\left(0.5-\frac{z}{h_b}\right)$

*

It is obvious to check from Table 1, UD and all of FG types will have the same value of volume fraction of CNTs. The mass density of nanotube reinforced composite is defined by $\rho = V_{CN}\rho^{CN} + V_m\rho^m$ [12]. The effective Poisson ratio depends weakly on position [9] and is described as follows:

$$\nu_{12} = V_{CN}^* \nu_{12}^{CN} + V_m \nu^m \tag{5}$$

2.1. First order shear deformation theory for face sheets

Based on First Order Shear Deformation, the strain components are described as follows:

$$\varepsilon_{xx}^i(x,z,t) = u_{,x}^i(x,z,t) = u_{0,x}^i(x,t) + z\phi_{,x}^i(x,t) \tag{6}$$

$$\gamma_{xz}^i(x,z,t) = u_{,z}^i(x,z,t) + w_{,x}^i(x,z,t) = \phi^i(x,t) + w_{0,x}^i(x,t) \tag{7}$$

The superscript (*i* = *t* or *b*) points to top and bottom face sheets, u^i_0 and w^i_0 are the mid plane displacement components in the *x* and *z* directions, and ϕ^i indicates the rotation of transverse normal line.

The stress–strain relations for the top and bottom face sheets based on linear elastic behaviour can be defined as [7]:

$$\begin{aligned} \sigma^i_{xx} &= E_{11}\varepsilon^i_{xx} \\ \tau^i_{xz} &= G_{13}\gamma^i_{xz} \end{aligned} \tag{8}$$

In which E_{11}, G_{13} are Young's modulus and shear modulus.

2.2. Core

The longitudinal and vertical displacement distributions of the core are approximated as quadratic and cubic polynomials in the transverse direction [10].

$$w^c(x,z,t) = w^c_0(x,t) + w^c_1(x,t)z_c + w^c_2(x,t)z^2_c \tag{9}$$

$$u^c(x,z,t) = u^c_0(x,t) + \varphi^c_0(x,t)z_c + u^c_2(x,t)z^2_c + u^c_3(x,t)z^3_c \tag{10}$$

In which $w_0{}^c(x, t)$ and $u_0{}^c(x, t)$ are the transverse and in-plane displacements and $\varphi_0{}^c(x,t)$ is the slope at the mid plane of the core. In the present sandwich beam theory, the core is perfectly bonded to the face sheets. Hence, transverse and in-plane compatibility conditions in top (*z* = -c/2), and bottom (*z* = c/2) interfaces should be satisfied as follows:

$$w^c(x,-\frac{c}{2},t) = w^t(x,t) \tag{11}$$

$$u^c(x,-\frac{c}{2},t) = u^t_0(x,t) + \frac{h_t}{2}\phi^t(x,t) \tag{12}$$

$$w^c(x,\frac{c}{2},t) = w^b(x,t) \tag{13}$$

$$u^c(x,\frac{c}{2},t) = u^b(x,t) - \frac{h_b}{2}\phi^b(x,t) \tag{14}$$

The strain components of the core based to linear strain-displacement relations are obtained as:

$$\begin{cases} \varepsilon^c_{xx}(x,z,t) = u^c_{,x}(x,z,t) \\ \gamma^c_{xz}(x,z,t) = u^c_{,z}(x,z,t) + w^c_{,x}(x,z,t) \\ \varepsilon^c_{zz}(x,z,t) = w^c_{,z}(x,z,t) \end{cases} \tag{15}$$

The transverse normal and shear stress–strain relations based on linear elastic behaviour can be defined as:

$$\begin{bmatrix}\sigma_{xx}^{c}\\ \sigma_{zz}^{c}\\ \tau_{xz}^{c}\end{bmatrix}=\begin{bmatrix}C_{11}^{c} & C_{13}^{c} & 0\\ C_{13}^{c} & C_{33}^{c} & 0\\ 0 & 0 & C_{55}^{c}\end{bmatrix}\begin{bmatrix}\varepsilon_{xx}^{c}\\ \varepsilon_{zz}^{c}\\ \gamma_{xz}^{c}\end{bmatrix} \tag{16}$$

Where C_{ij}^{c} (*i, j* = 1, 3, 5) are stiffness coefficients for orthotropic materials. The stress- displacement relations can be expressed by inserting the strain-displacement relations in Eq. (16). This in turn, all strain and stress components resulted in terms of displacements.

2.3. Governing equations

The Ritz method is adopted to derive governing equations of equilibrium from total potential energy function of the sandwich beam. The total potential energy (Π) includes the strain energy (U), kinetic energy (T) and the potential external forces.

$$\prod = U + T - W \tag{17}$$

The strain energy includes two parts: strain energy of the face sheets (U_f) and strain energy of the core (U_c) as follows:

$$U = U_f + U_c \tag{18}$$

The strain energy of the sandwich beam that consists of energetically conjugate pairs of stress and strain of face sheets and core, is given by:

$$U_f = \int_{V_t}\left(\int \sigma_{xx}^{t} d\varepsilon_{xx}^{t} + K_s \int \tau_{xz}^{t} d\gamma_{xz}^{t}\right)dv_t + \int_{V_b}\left(\int \sigma_{xx}^{b} d\varepsilon_{xx}^{b} + K_s \int \tau_{xz}^{b} d\gamma_{xz}^{b}\right)dv_b \tag{19(a)}$$

$$U_c = \int_{V_c}\left(\int \sigma_{xx}^{c} d\varepsilon_{xx}^{c} + \int \sigma_{zz}^{c} d\varepsilon_{zz}^{c} + \int \tau_{xz}^{c} d\gamma_{xz}^{c}\right)dv_c \tag{19(b)}$$

Where V_t, $V_b$and V_c refers to volumetric domains of the top and bottom face sheets and the core, respectively.

The kinetic energy includes three parts: kinetic energy of the face sheets (T_f), kinetic energy of the core (T_c) and kinetic energy of the impactor as follows:

$$\begin{aligned}
T_f &= \int_{V_t}\left(\frac{1}{2}\rho_t\left((\dot{u}(x,z,t))^2 + \dot{w}(x,z,t)^2\right)\right)dv_t + \int_{V_b}\left(\frac{1}{2}\rho_b\left((\dot{u}(x,z,t))^2 + \dot{w}(x,z,t)^2\right)\right)dv_b\\
T_c &= \int_{V_c}\left(\frac{1}{2}\rho_c\left((\dot{u}(x,z,t))^2 + \dot{w}(x,z,t)^2\right)\right)dv_c\\
T_{imp} &= \frac{1}{2}M_{imp}\dot{w}_p^2
\end{aligned} \tag{20}$$

where (.) denote to derivative respected to time and ρ_c is density of the core. Also, ρ_t and ρ_b denote to density of top and bottom face sheets, respectively. Also, M_{imp} stands for the mass of the impactor.

Assuming that Hertz contact law governs the relation of contact force and indentation, the potential energy of the contact force is equal to:

$$W = \frac{2}{5}K_{imp}(w_p - w_t(x_{imp},t))^{5/2} \tag{21}$$

where in the above equation x_{imp} is the position in which impact takes place, w_p is the displacement of the impactor and α indicates the indentation in the top face sheet which is replaced by $\alpha = w_p - w_t(x_{imp},t)$. $K_{imp}$is the contact stiffness which is evaluated by Wang *et al.* [12].

$$K_i = \frac{4}{3}\sqrt{R}\left(\frac{1}{E_{33,imp}} + \frac{1-\nu_s^2}{E_s}\right)^{-1} \tag{22}$$

In the above equation, ν_s and E_s are the Poisson ratio and elasticity modulus of the impactor and $E_{33,imp}$is the transverse elasticity modulus in the surface of FG–CNTRC top face sheet where impact occurs.

Finally, by inserting Eqs. (19), (20) and (21) into generalised Lagrange Equations, the governing equations of elastic analysis can be derived as follows:

$$\begin{aligned} &\frac{d}{d_t}\left(\frac{\partial T_c}{\partial \dot{Q}_j^i}\right) + \frac{d}{d_t}\left(\frac{\partial T_f}{\partial \dot{Q}_j^i}\right) + \frac{d}{d_t}\left(\frac{\partial T_{imp}}{\partial \dot{Q}_j^i}\right) + \frac{\partial U_c}{\partial Q_j^i} + \frac{\partial U_f}{\partial Q_j^i} + \frac{\partial W}{\partial Q_j^i} = 0 \\ &\left\{Q_j^i\right\} = \begin{Bmatrix} \left\{U_{0j}^t\right\}, \left\{\Phi_j^t\right\}, \left\{W_{0j}^t\right\}, \left\{U_{0j}^b\right\}, \left\{\Phi_j^b\right\}, \left\{W_{0j}^b\right\}, \\ \left\{U_{0j}^c\right\}, \left\{\Phi_{0j}^c\right\}, \left\{W_{0j}^c\right\} \end{Bmatrix}, j = 1,..,M \end{aligned} \tag{22}$$

The resulted equations from (22) are a system of 9M second order differential equations in time domain and can be expressed in the compact matrix form as follows:

$$\begin{aligned} &[M]\left\{\ddot{Q}\right\} + [K]\left\{Q^i\right\} = \left\{F\right\} \\ &M_{imp}\ddot{w}_p = F_{imp} \end{aligned} \tag{23}$$

Where [*K*] is a coefficient matrix (or stiffness matrix), [*M*] is the mass matrix and {*F*} is a forcing vector.

Also, F_{imp} may be represented in terms of the newly defined shape functions as:

$$\begin{aligned} &F_{imp} = K_{imp}\left(w_p - \mathrm{R}_\delta \sum_{j=1}^{M} W_{0j}^t P_j(\xi_{imp})\right)^{3/2} \\ &\xi_{imp} = \frac{2x_{imp}}{l} \end{aligned} \tag{24}$$

There are several numerical integration methods available to integrate second order equations in time domain. In this study, the resulted time-dependent equations are then solved via the fourth-order Runge–Kutta method.

3. Results and Discussion

In this section, the numerical results based on above procedure are presented to study impact response of a sandwich beam with FG–CNTRC face sheets and soft core. Generally, the material properties of CNTRC face sheets are explained in reference [10]. The efficiency parameters are chosen to equal the obtained magnitudes of E_{11} and G_{12} from the proposed modified rule of mixture with those obtained by Han and Elliott [1].

3.1. Comparison study

The central displacement history of the top face sheet of a simply supported isotropic sandwich beam is computed from the present approach and compared with the one evaluated by Qiao *et al* [6]. The results reveal that the peaks of the central transverse displacement of the top face sheet based on present theory are higher (Figure 2). This is because that the results of Qiao *et al.* [6] were achieved based on HSAPT in which the face sheets follow the classical beam theory.

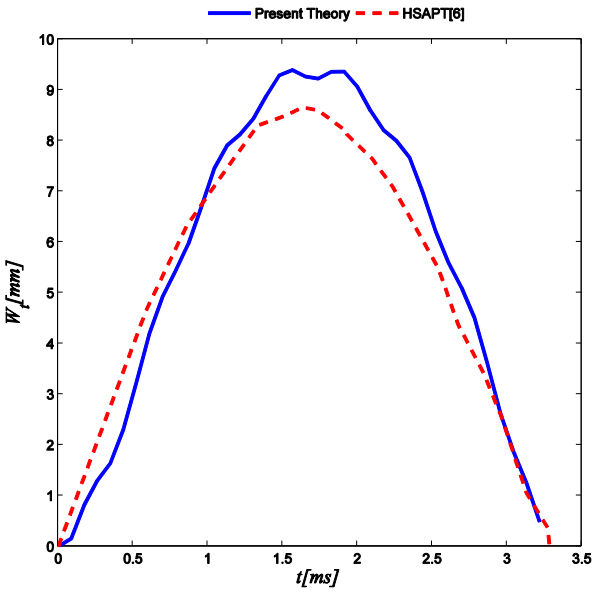

Figure 2. A comparison on central displacement history of the top face sheet for sandwich beam with isotropic face sheets

3.2. Parametric study

Low velocity impact characteristics of sandwich beams with CNTRC face sheets and soft core are studied. Polyurethane soft foam is selected as a soft core. The material properties of the core are E_c = 217 [MPa], G_c = 76 [MPa] and ρ_c = 210 kg/m^3 [3]. The CNTRC face sheets are carried out based on the material properties for the reference temperature (T_0 = 300 K) [11]. Geometrical characteristics of the sandwich beam are length L = 60 mm, width b = 10mm and thickness of the face sheets $h_t = h_b$ = 1 mm. In this study, the core-to-face sheet thickness ratio are c/h_t = 4, 6 and 8. Impactor is made from steel with material properties E_s = 207 GPa, ρ_s = 7,960 kg/m^3 and υ_s = 0.5. Unless otherwise stated, a spherical impactor with radius R_{imp} = 10 mm and initial velocity V_{imp} = 3 m/s is impacting the target at the midspan of the beam, i.e., $x_{imp} = L/2$. In the next, only a sandwich beam with both edges simply supported is analysed since generally the required time for the stress wave to travel to boundary and reflect back is less than the low velocity impact event time.The effects of distribution of CNTs, core-to-face sheet thickness ratio, initial velocity of the impactor and the impactor mass are studied in detail.

3.2.1. Case I: Influence of graded profile of CNTs

The effects of three types of grading profiles, namely, UD, FG-V and FG-Λ on contact force history and the indentation of the impactor are depicted in Figure 3. As may be readily noted from Figure 3, the case of FG-V has the least contact time and the most peak contact force. The case of FG-Λ, on the other hand, has the minimum peak contact force and the highest contact time due to its lowest transverse Young moduli at the impacted layer of the top face sheet. Besides, stiffness of the impacted

section affects the time instant corresponding to the maximum contact force. As a result, the time instant associate with the stiffer impacted section becomes smaller. The indentation of the impactor in the sandwich beam is maximum for FG-Λ, followed by UD and FG-V. It is worth-noting that, contact stiffness for different grading profiles are different due to different volume fraction of CNTs at the impact surface. Due to this reason, maximum contact force and maximum indentation do not belongs to the same case of grading profile. The maximum contact stiffness among the three grading profiles belong to the case of FG-V grading. As may be concluded, by decreasing the volume fraction of the CNTs at outer surfaces, the sandwich panel becomes softer. As a result, the FG-Λ CNTRC face sheet gives the most flexibility to the sandwich beam among the other types.

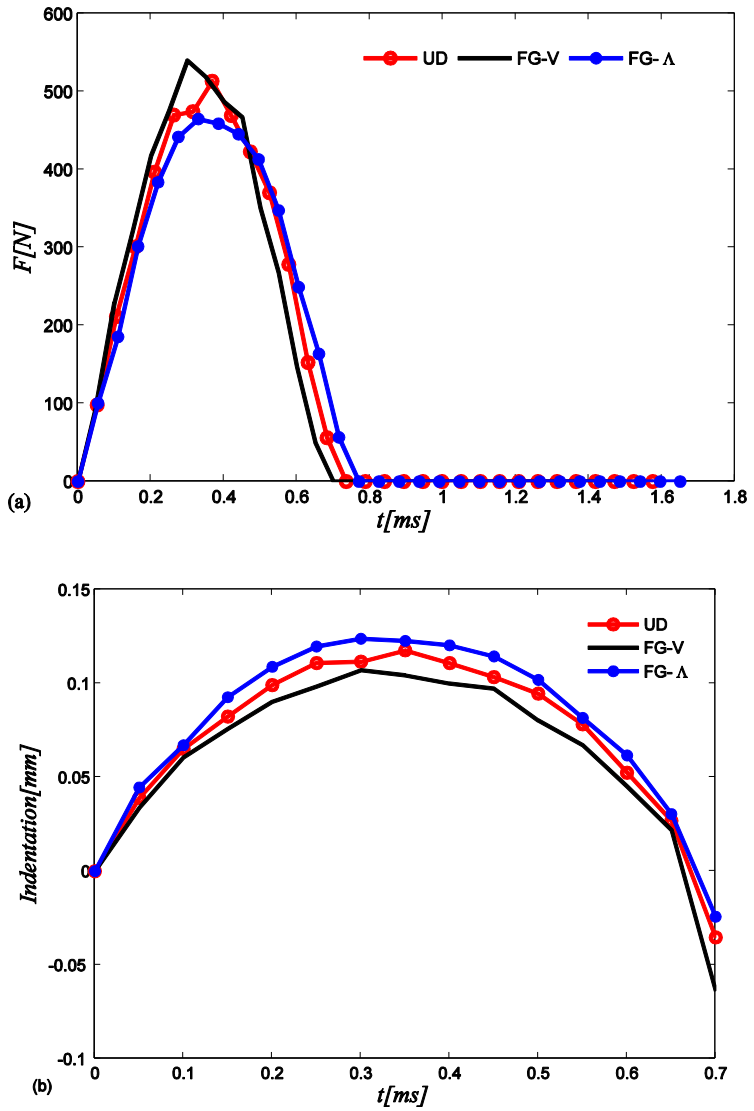

Figure 3. The influence of distribution pattern of CNTRC on low velocity impact responses at the midspan point of the top face: (a) contact force history (b) indentation

3.2.2. Case II: Influence of the core-to-face sheet thickness ratio (c/ht)

The effect of core-to-face sheet thickness ratio (c/h_t) on the low velocity response of FG-V sandwich beam is indicated in Figure 4. Since the thickness of the face sheets are kept constant, therefore, the

increasing c/h_t involving thicker cores. As thicker the core is, the higher the flexural stiffness of the sandwich panel is.

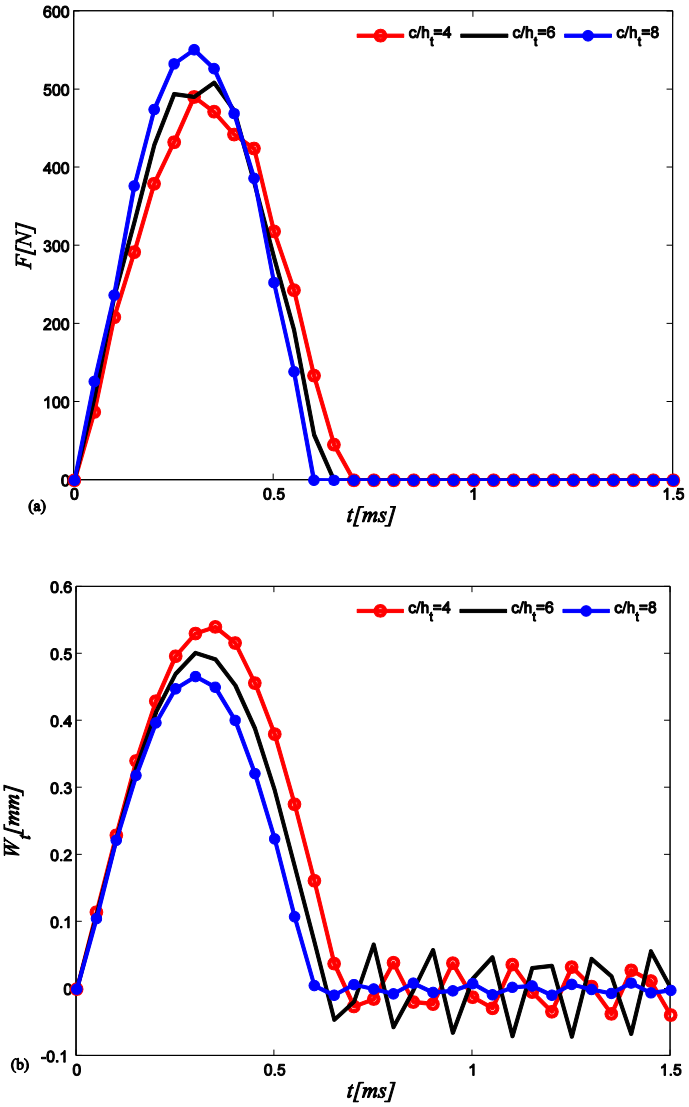

Figure 4 The effect of core-to-face sheet thickness ratio (c/h_t) on low velocity impact responses at the midspan point of the top face: (a) contact force history (b) transverse displacement

3.2.3. Case III: Influence of impactor's mass

Present section aims to analyse the low velocity impact response of a sandwich beam with FG–CNTRC face sheets subjected to various impactors of different masses. Initial velocity of the impactor is chosen as V_{imp} = 3 m/s. Three different values are considered for the impactor radius that are R_{imp} = 10, 11 and 12 mm. As expected, results depicted in Figure 5 reveals that as the initial kinetic energy of the impactor increases, the contact forces and central displacement of the top face sheet increase. However, if the increase in the kinetic energy of the impactor has occurred due to an increased impactor mass, the contact time will be higher otherwise it will be lower in comparison the initial contact time.

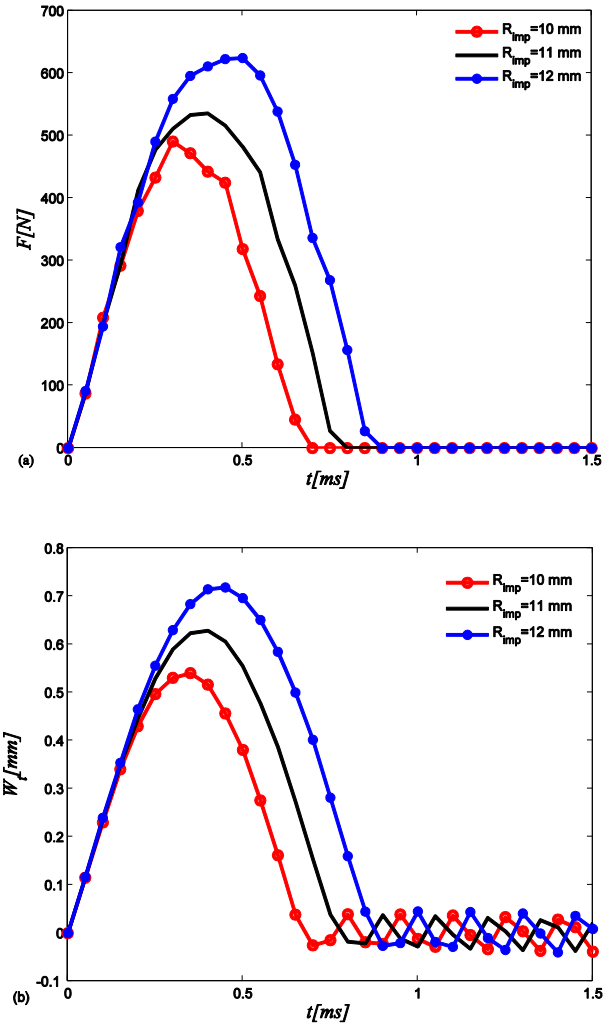

Figure 5. Influence of the mass of the impactor on low velocity impact responses at the midspan point of the top face: (a) contact force history (b) transverse displacement

4. Conclusion

In this study, response of sandwich beam with CNTRC face sheets and soft cores subjected to the action of an impacting mass is presented. Generally, the numerical results reveal that:

- Generally, it is concluded that, whenever the outer surface of the CNTRC face sheet is CNT-rich, the face sheet becomes stronger and results in higher peak contact force and lower transverse displacement of the top face sheet in sandwich beams with CNTRC faces and soft cores.
- The numerical results reveal that the sandwich beam with the FG–CNTRC face sheets has lower deflection along with higher contact force when it has a higher core-to-face sheet thickness ratio. Also, due to increasing the flexural stiffness of the sandwich panel by increasing the c/h_t, the central displacement of the top face sheet is decreased.
- As one may conclude, the higher impactor radius is the higher mass and inertia of the impactor is. Therefore, increasing the inertia of the impactor results in higher contact time duration.

References

[1] Y. Han and J. Elliott, "Molecular dynamics simulations of the elastic properties of polymer/carbon nanotube composites," *J. Comput. Mater. Sci*., vol. 39, pp. 315–323, 2007.

[2] S. Jedari Salami *et al*., "Improved extended high order analysis of sandwich beams with a bilinear core shear behavior," *J. Sandwich Struct. Mater.*, vol. 16, pp. 633–668, 2014.

[3] S. Jedari Salami, "Extended high order sandwich panel theory for bending analysis of sandwich beams with carbon nanotube reinforced face sheets," *Physica E: Low Dimensional Sys. Nanostruct*., vol. 76, pp. 87–197, 2016.

[4] S. Jedari Salami, "Dynamic extended high order sandwich panel theory for transient response of sandwich beams with carbon nanotube reinforced face sheets," *Aero. Sci. Tech.* vol. 56, pp. 56–69, 2016.

[5] K. M. Liew *et al.*, "Mechanical analysis of functionally graded carbon nanotube reinforced composites: a review," *Compos. Struct*., vol. 120, pp. 90–97, 2015.

[6] P. Qiao, and M. Yang, "Impact analysis of fiber reinforced polymer honeycomb composite sandwich beams," *Compos. Part B Eng*., vol.38, pp. 739–750, 2007.

[7] J. N. Reddy, *Mechanics of laminated composite plates and shells: theory and analysis*, 2nd ed. Boca Raton, Florida: CRC Press, 2003.

[8] H. S. Shen, "Nonlinear bending of functionally graded carbon nanotube reinforced composite plates in thermal," *Compos. Struct*., vol. 91, pp. 9–19, 2009.

[9] H. S. Shen, "Postbuckling of nanotube-reinforced composite cylindrical shells in thermal environments, part I: axially-loaded shells," *Compos. Struct*., vol. 93, pp. 2096–2108, 2011.

[10] H. S. Shen, and Y. Xiang, "Nonlinear bending of nanotube reinforced composite cylindrical panels resting on elastic foundations in thermal environments," *Eng. Struct*., vol. 80, pp. 163–172, 2014.

[11] H. S. Shen and Y. Xiang, "Postbuckling of nanotube-reinforced composite cylinderical shells under combined axial and radial mechanical loads in thermal environment," *Compos. Part B Eng.*, vol. 52, pp. 311–322, 2013.

[12] Z. X. Wang *et al.*, "Nonlinear low-velocity impact analysis of temperature-dependent nanotube-reinforced composite plates," *Compos. Struct*., vol. 106, pp. 423–434, 2014.